A Performance Study for Two Current Sensor Free Single-Cell Maximum Power Point Tracking Methods for High Performance Vehicle Solar Arrays

Peter Wolfs
Faculty of Sciences, Engineering and Health
Central Queensland University
Rockhampton, Queensland, Australia
p.wolfs@cqu.edu.au

Quan Li
Faculty of Sciences, Engineering and Health
Central Queensland University
Rockhampton, Queensland, Australia
q.li@cqu.edu.au

ABSTRACT

Two Maximum Power Point Tracking (MPPT) control algorithms have been previously developed for the single high performance dual junction or triple junction solar cells for hybrid and electric vehicle applications. These algorithms are respectively based on the Perturb and Observe (P&O) and the Incremental Conductance (IncCond) methods but remove the need for current sensing devices. This paper provides a comparison of the two MPPT control algorithms and a detailed performance evaluation of the two algorithms under both static and dynamic tests. The Incremental Conduction algorithm achieved slightly better results and static tracking accuracy of 99% .

1. INTRODUCTION

The declining production of the fossil fuels, together with the environmental concerns, has drawn increasing interests in hybrid and electric vehicles on the global automotive market. With the advancement of the photovoltaic (PV) technology, solar arrays may become viable in providing a useful energy input for the hybrid and electric vehicles. Unlike that for other terrestrial PV applications, MPPT for vehicle solar arrays will require highly efficient solar cells and highly distributed maximum power trackers due to limited area, curved surface and rapid insolation changes.

Two cost-effective MPPT control algorithms based on the conventional Perturb and Observe (P&O) and Incremental Conductance (IncCond) methods have been previously proposed for the applications in high performance vehicle solar arrays [1], [2]. Figure 1 shows the prototype Maximum Power Point Tracker with an Emcore triple junction solar cell [3]. The MPPT hardware employs a buck converter controlled by Texas instrument MSP430 microprocessor [4]. The proposed MPPT control algorithms are able to establish the Maximum Power Point (MPP) based on the solar cell voltage and the converter switching duty ratio alone therefore current sensing devices are no longer required.

This paper first provides a comparison of the two MPPT current-sensor-free control algorithms. Then the performances of the two MPPT control algorithms under instantaneous insolation changes are studied in detail. Both static and dynamic tests are conducted under instantaneous insolation changes between three insolation levels including full sun, half sun and 10% sun. The experimental waveforms are shown and discussions on the two MPPT control algorithms are provided at the end of the paper.

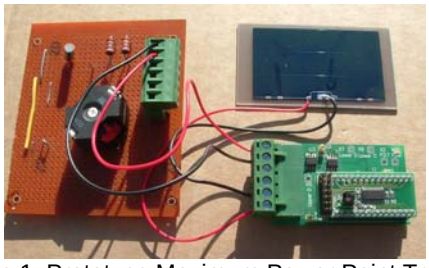

Figure 1: Prototype Maximum Power Point Tracker

2. TWO CURRENT-SENSOR-FREE MPPT CONTROL ALGORITHMS

To date, two popular MPPT control algorithms are P&O method and IncCond method [5]-[10]. These two methods require the measurement of both the solar cell voltage and current in order to establish the MPP and they are not suited for highly distributed MPPT scheme, where the power rating of the individual Maximum Power Point Trackers may fall in the milliwatt range.

The two improved methods remove the need of the current measurement. Figure 2 shows the simplified control block diagram, where $V_{ref}(k)$ and $V_{ref}(k+1)$ are respectively the demanded cell voltage in the kth and the (k+1)th MPPT cycles, v_{cell} is the measured cell voltage, D is the buck converter switching duty ratio and C_v is a constant whose sign is determined by the MPPT controller calculation result. Table 1 shows the comparison of the two control methods. It is worth mentioning that these two approaches can be applied to any load characteristic where the output voltage increases monotonically with the output power.

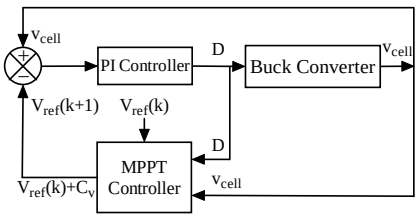

Figure 2: MPPT control block diagram

Method	P&O	IncCond
Input	Cell voltage v_{cell} and switching duty ratio D	Cell voltage v_{cell} and switching duty ratio D
MPP Equation	The MPP equation does not exist.	$D + v_{cell}\, dD/dv_{cell} = 0$
$C_V > 0$	$[v_{cell}(k+1) - v_{cell}(k)][D(k+1)v_{cell}(k+1) - D(k)v_{cell}(k)] > 0$	$D(k+1) + v_{cell}(k+1)\frac{D(k+1) - D(k)}{v_{cell}(k+1) - v_{cell}(k)} > 0$
$C_V < 0$	$[v_{cell}(k+1) - v_{cell}(k)][D(k+1)v_{cell}(k+1) - D(k)v_{cell}(k)] < 0$	$D(k+1) + v_{cell}(k+1)\frac{D(k+1) - D(k)}{v_{cell}(k+1) - v_{cell}(k)} < 0$
Oscillation	The operating point oscillates around MPP as the cell voltage is constantly perturbed.	The operating point does not oscillate around MPPT as the MPPT calculation is bypassed once MPP is reached.
Deviation	The operating point may deviate from MPP under rapidly and uni-directionally changing atmospheric conditions.	The operating point does not deviate from MPP.

Table 1: Comparison of the two current-sensor-free MPPT control algorithms

3. SOLAR CELL SIMULATOR

In order to provide controlled insolation levels and rapid insolation changes, a solar cell simulator is made with a switchable current source and several shunting resistances and diodes [1]. To evaluate the performances of the two proposed MPPT control algorithms, the current-voltage and the power-voltage characteristics of the solar cell simulator are obtained through the capacitance load test. In this test, a capacitor is employed as the only load of the solar cell simulator and is charged from the short circuit condition where the cell provides zero voltage and maximum current to the open circuit condition where the cell provides maximum voltage and zero current. The capacitor voltage and current waveforms are captured by a digital oscilloscope during the entire process and finally transformed to the cell characteristic curves. An important feature of the test is that it offers a direct and accurate foundation for the tracking performance evaluations in due course.

The solar cell simulator is designed to model the Emcore triple junction cell under three insolation levels including full sun, half sun and 10% sun [3]. The current-voltage and the power-voltage curves are shown in Figures 3 and 4, where the solid lines represent the solar cell simulator curves under full sun, the dashed lines represent that under half sun and the dashed-dotted lines represent that under 10% sun. The cell voltage, current and power at the MPPs obtained from Figures 3 and 4 under three insolation levels are given in Table 2.

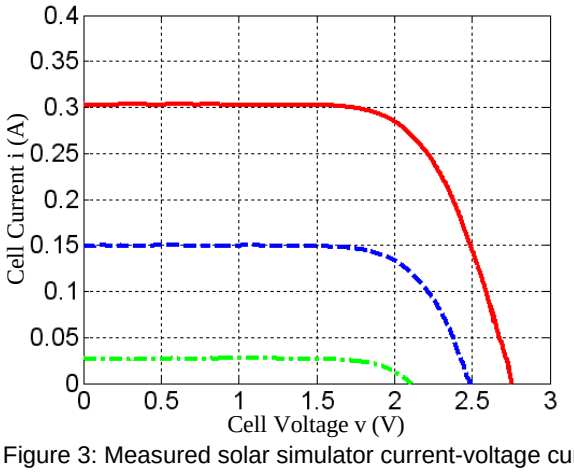

Figure 3: Measured solar simulator current-voltage curve

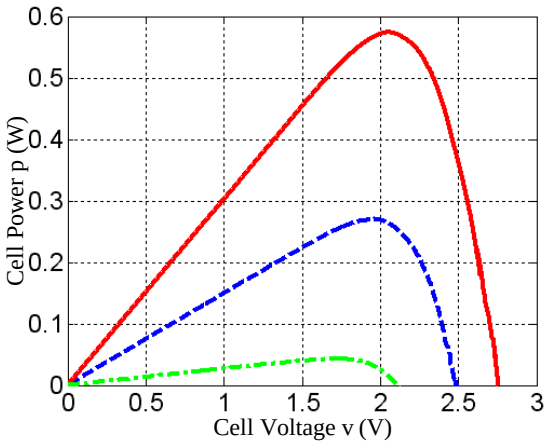

Figure 4: Measured solar simulator power-voltage curve

Insolation	Voltage (V)	Current (A)	Power (W)
Full Sun	2.058	0.279	0.574
Half Sun	1.967	0.137	0.270
10% Sun	1.729	0.025	0.043

Table 2: Maximum Power Points under three insolation levels

4. EXPERIMENTAL WAVEFORMS

In order to verify the theoretical analysis, the buck converter is loaded with the corresponding MPPT control algorithms and connected to a load consisting of 2500-μH inductor and a 4.1-Ω resistor. The experimental waveforms under instantaneous insolation changes between half and full sun and between 10% and full sun are respectively provided for the individual control methods.

4.1. P&O ALGORITHM

Figures 5 and 6 respectively show the experimental waveforms of the P&O algorithm under instantaneous insolation step-up from half to full sun and from 10% to full sun. Figures 7 and 8 respectively show the experimental waveforms of the P&O algorithm under instantaneous insolation step-down from full to half sun and from full to 10% sun. From top to bottom, Figures 5 to 8 respectively shows the cell voltage, the converter output midpoint to ground voltage, the cell current and the load current. While the establishment of the new MPP is largely complete in 1.5 ms when the insolation

changes instantaneously between half and full sun, it does take longer to establish the new MPPs when the insolation changes instantaneously between 10% and full sun. In the latter case, the establishment of the new MPP under the step-up or step-down changes is largely complete in 2 ms or 5 ms.

As the insolation step-up transition and step-down transition respectively fall in the semi-constant voltage and semi-constant current regions on the current-voltage curve, the cell current present different patterns in the experimental waveforms shown in Figures 5 to 8.

The current voltage loci when the insolation steps up from half to full sun and steps down from full to half sun are respectively shown by the solid lines in Figures 9 and 10.

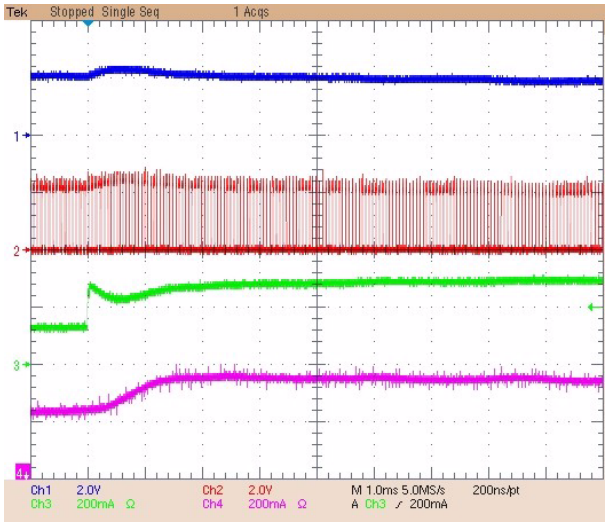

Figure 5: Experimental waveforms – from half to full sun, Trace 1 – Cell Voltage; Trace 2 Converter Output; Trace 3 Cell Current; Trace 4 Load Current.

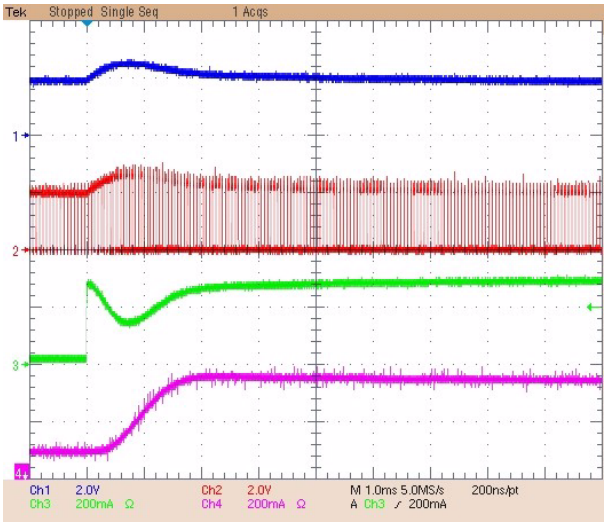

Figure 6: Experimental waveforms – from 10% to full sun Trace 1 – Cell Voltage; Trace 2 Converter Output; Trace 3 Cell Current; Trace 4 Load Current.

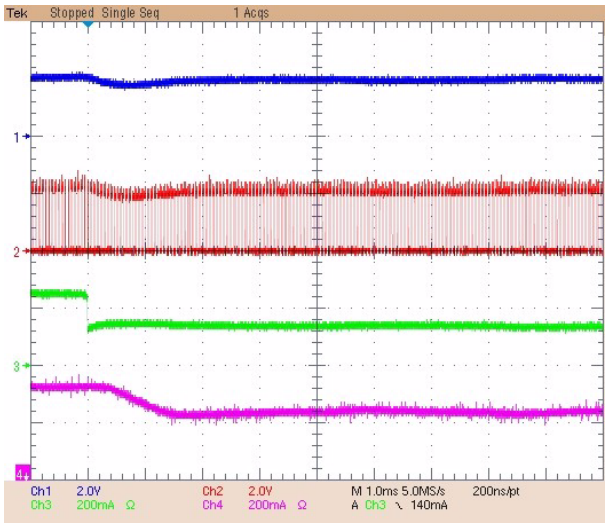

Figure 7: Experimental waveforms – from full to half sun

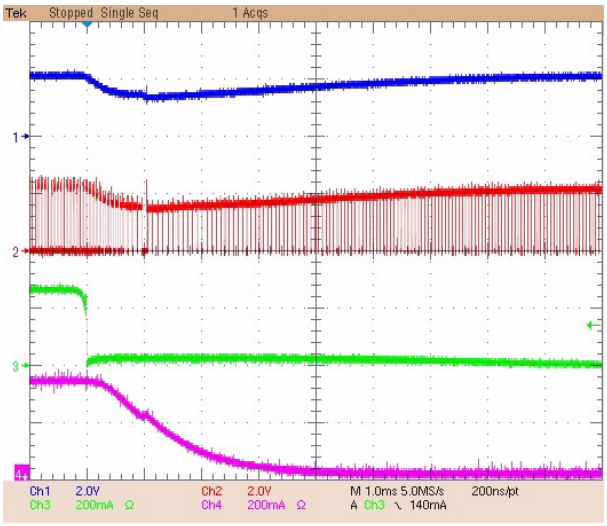

Figure 8: Experimental waveforms – from full to 10% sun

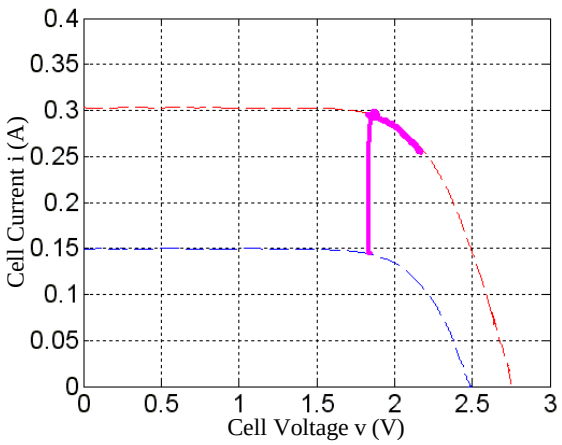

Figure 9: Current voltage loci over insolation step-up

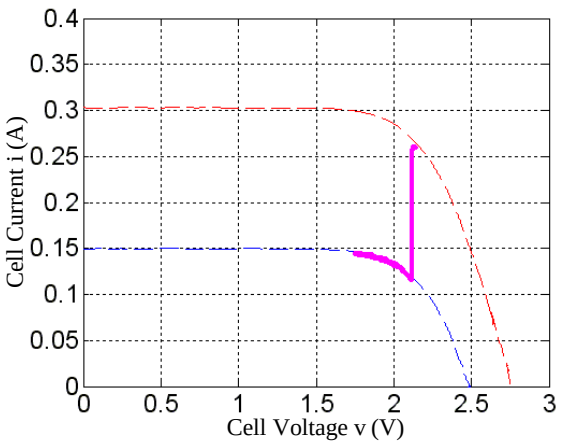

Figure 10: Current voltage loci over insolation step-down

4.2. INCCOND ALGORITHM

Figures 11 and 12 respectively show the experimental waveforms of the IncCond algorithm under instantaneous insolation step-up from half to full sun and from 10% to full sun. Figures 13 and 14 respectively show the experimental waveforms of the IncCond algorithm under instantaneous insolation step-down from full to half sun and from full to 10% sun. From top to bottom, Figures 11 to 14 respectively shows the cell voltage, the converter output midpoint to ground voltage, the cell current and the load current. These waveforms are similar to those under P&O algorithm.

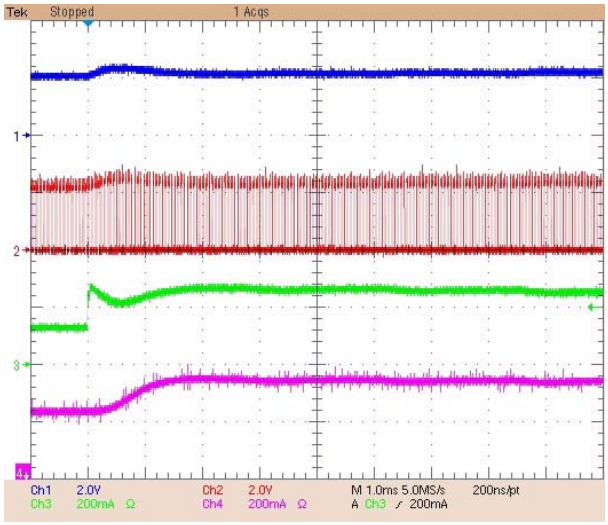

Figure 11: Experimental waveforms – from half to full sun Trace 1 – Cell Voltage; Trace 2 Converter Output; Trace 3 Cell Current; Trace 4 Load Current.

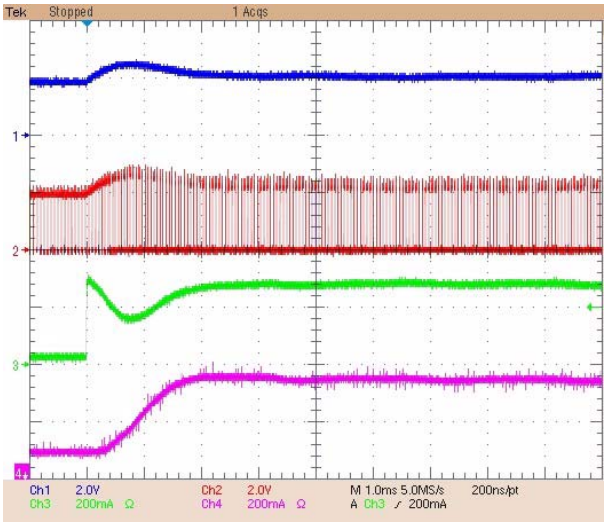

Figure 12: Experimental waveforms – from 10% to full sun Trace 1 – Cell Voltage; Trace 2 Converter Output; Trace 3 Cell Current; Trace 4 Load Current.

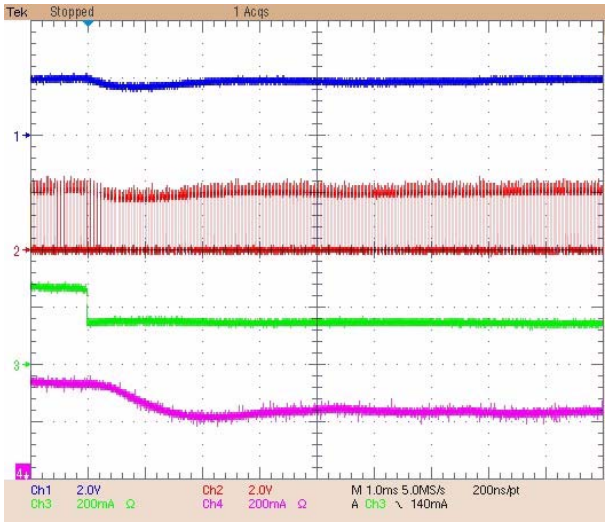

Figure 13: Experimental waveforms – from full to half sun

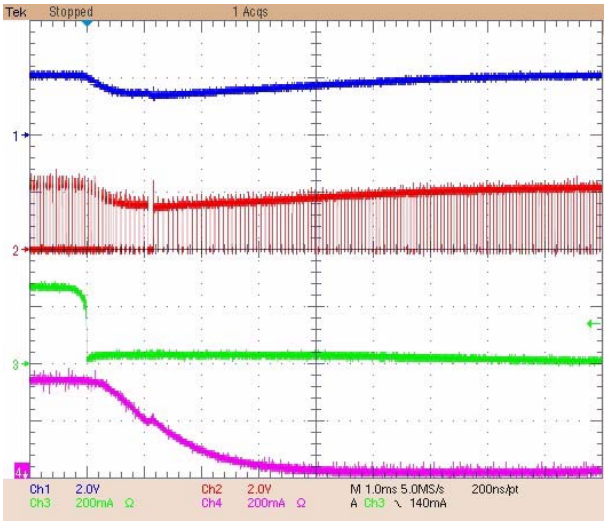

Figure 14: Experimental waveforms – from full to 10% sun

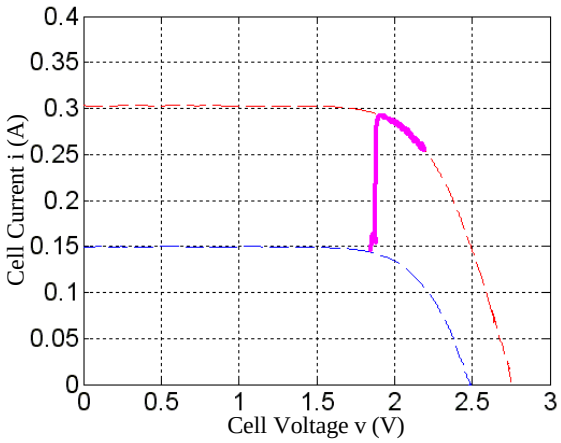

Figure 15: Current voltage loci over insolation step-up

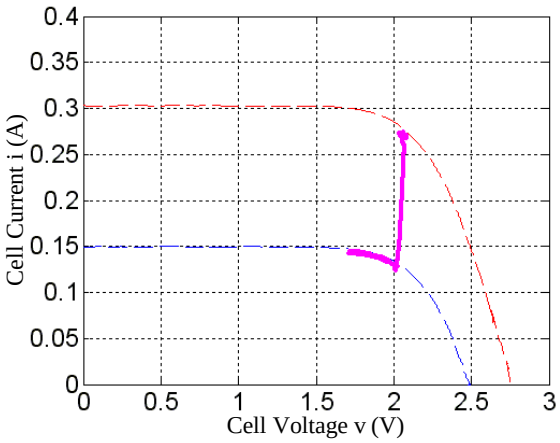

Figure 16: Current voltage loci over insolation step-down

The current voltage loci when the insolation steps up from half to full sun and steps down from full to half sun are respectively shown by the solid lines in Figures 15 and 16.

5. TRACKING PERFORMANCE EVALUATIONS

In order to evaluate the tracking performance of the two MPPT control algorithms, both static and dynamic tests are conducted. In the static test, the cell voltage, current and power are measured under the individual insolation levels. In the dynamic test, the waveform of the power is recorded for the period between 1 ms before and 2 ms after the insolation changes between half and full sun and between 10% and full sun.

5.1. P&O ALGORITHM

The measured static MPP conditions for P&O algorithm are given in Table 3. It can be seen that the actual cell output powers under full and half sun are above 97% of the corresponding maximum available cell powers given in Table 2 while the cell output power under 10% sun is only 81% of the maximum available cell power given in Table 2.

Insolation	Voltage (V)	Current (A)	Power (W)
Full Sun	2.054	0.274	0.560
Half Sun	1.940	0.137	0.266
10% Sun	1.906	0.018	0.035

Table 3: Maximum Power Points under three insolation levels – P&O Algorithm

Figures 17 and 18 respectively show the cell output power waveform for the P&O algorithm when the insolation steps up instantaneously from half to full sun and from 10% to full sun. Figures 19 and 20 respectively show the cell output power for the P&O algorithm when the insolation steps down instantaneously from full to half sun and from full to 10% sun. In Figures 17 to 20, the solid lines represent the actual cell power, the dashed lines represent the maximum available cell power and the dashed-dotted lines represent 90% of the maximum available cell power.

5.2. INCCOND ALGORITHM

The measured static MPP conditions under IncCond algorithm are given in Table 4. It can be seen that the actual cell output powers under three insolation conditions including full, half and 10% sun are all above 99% of the corresponding maximum available cell powers given in Table 2.

Insolation	Voltage (V)	Current (A)	Power (W)
Full Sun	2.058	0.276	0.569
Half Sun	1.952	0.138	0.269
10% Sun	1.787	0.025	0.043

Table 4: Maximum Power Points under three insolation levels – IncCond Algorithm

Figures 21 and 22 respectively show the cell output power for the IncCond algorithm when the insolation steps up instantaneously from half to full sun and from 10% to full sun. Figures 23 and 24 respectively show the cell output power for the IncCond algorithm when the insolation steps down instantaneously from full to half sun and from full to 10% sun. In Figures 21 to 24, the solid lines represent the actual cell power, the dashed lines represent the maximum available cell power and the dashed-dotted lines represent 90% of the maximum available cell power.

5.3. COMPARISON

In the static test, the measured MPP conditions under two different MPPT control algorithms shown in Tables 3 and 4 respectively agree with those shown in Table 2. The MPP conditions under the IncCond algorithm are slightly more accurate than those under the P&O algorithm and this is especially true under the low insolation level of 10% sun.

It can be observed in the dynamic tests, Figures 17 to 24, that when the insolation has a step change between half and full sun or a step-down from full to 10% sun, the actual cell powers are largely controlled above 90% of the new maximum available cell powers during transition period for both MPPT control algorithms. When the insolation steps up instantaneously from 10% to full sun, the actual power reaches 90% of the new maximum available cell power in 1.5 ms for the P&O algorithm and in 1.2 ms ufor the IncCond algorithm.

The energy loss related to the difference between the actual and maximum available cell powers in 2 ms after the insolation changes are calculated for the P&O and the IncCond algorithms and listed in Table 5. It can be observed that while the energy losses under the IncCond algorithm are comparable to those under the P&O algorithm during insolation step-down, the energy losses under the IncCond algorithm are less than 50% of those under the P&O algorithm during insolation step-up. Therefore, the dynamic response of the IncCond algorithm is also slightly better than that of the P&O algorithm.

Insolation Change		Energy Loss for P&O (mJ)	Energy Loss for IncCond (mJ)
Full and Half Sun	Step-Up	0.065	0.028
	Step-Down	0.014	0.021
Full and 10% Sun	Step-Up	0.213	0.106
	Step-Down	0.010	0.014

Table 5: Energy Loss in 2 ms after the Insolation Change under Two MPPT Control Algorithms

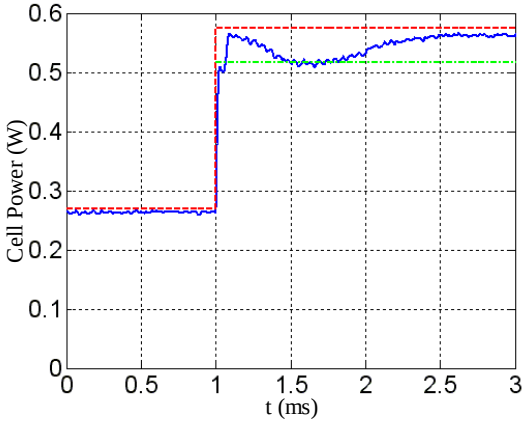

Figure 17: Cell power over step-up from half to full sun

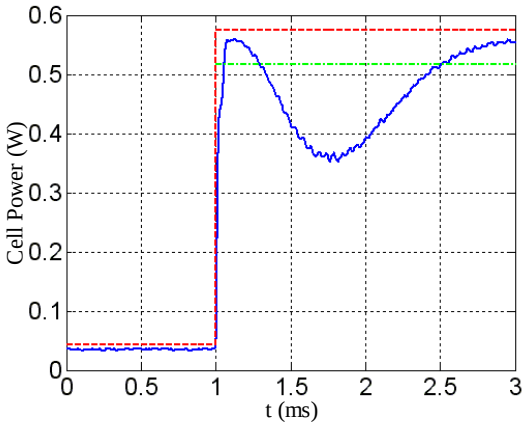

Figure 18: Cell power over step-up from 10% to full sun

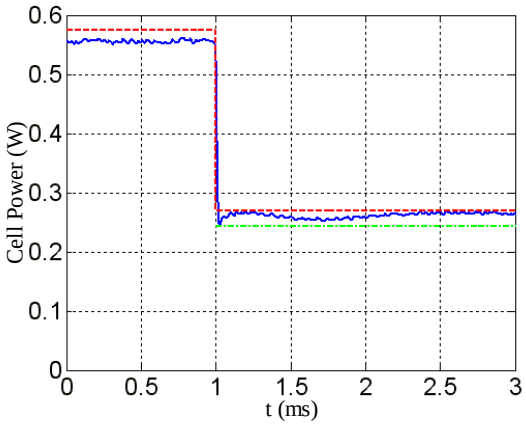

Figure 19: Cell power over step-down from full to half sun

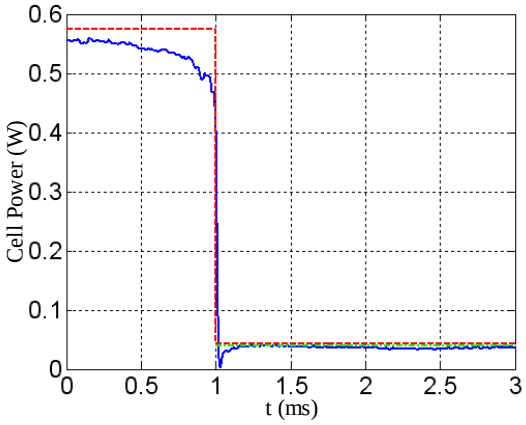

Figure 20: Cell power over step-down from full to 10% sun

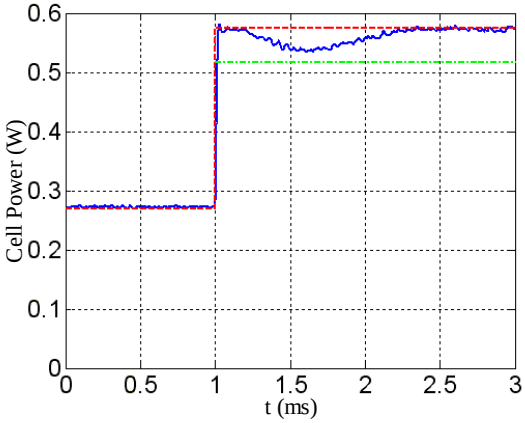

Figure 21: Cell power over step-up from half to full sun

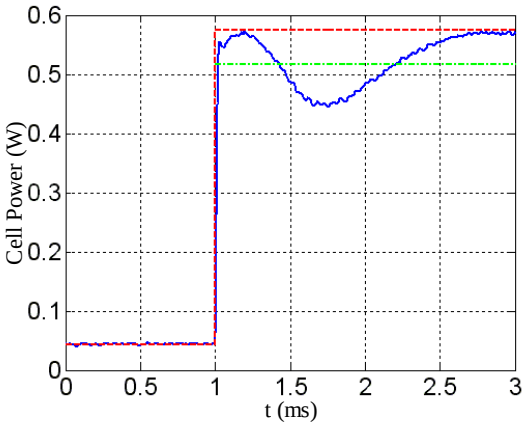

Figure 22: Cell power over step-up from 10% to full sun

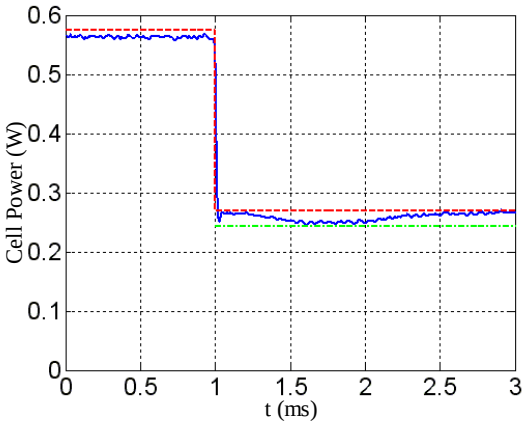

Figure 23: Cell power over step-down from full to half sun

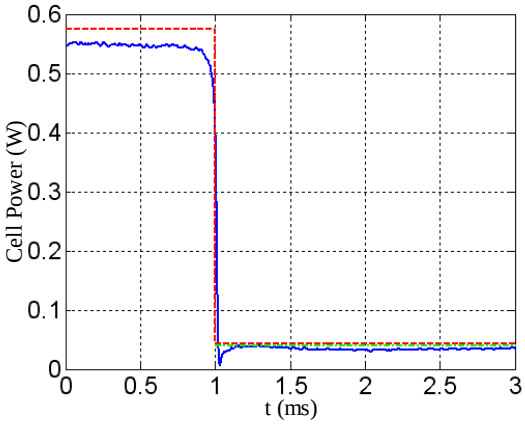

Figure 24: Cell power over step-down from full to 10% sun

6. CONCLUSIONS

This paper provides a detailed performance study of the two current-sensor-free MPPT control algorithms based on the P&O and the IncCond methods. The experimental waveforms of the two algorithms are shown for instantaneous insolation changes between 10% and full sun and half and full sun. The tracking performance is also conducted for the two MPPT algorithms under both static and dynamic tests. It can be established that the IncCond algorithm has better performance in tracking the rapid changing insolation conditions. As the IncCond offers another two features including oscillation-free at the MPP and no deviation from the MPP under rapidly and uni-directionally changing insolation conditions, it will be employed as the final version of the MPPT controller for the high performance vehicle solar arrays.

7. ACKNOWLEDGEMENTS

This work was supported by the Queensland Department of Public Works and Housing and the Queensland Department of Transport.

REFERENCES

[1] P. Wolfs and L. Tang, "A Single Cell Maximum Power Point Tracking Converter without a Current Sensor for High Performance Vehicle Solar Arrays," in *Proc. IEEE PESC*, 2005, pp. 165-171.

[2] P. Wolfs and Q. Li, "A Current-Sensor-Free Incremental Conductance Single Cell MPPT for High Performance Vehicle Solar Arrays," in *Proc. IEEE PESC*, 2006, pp. 117-123.

[3] Emcore Corporation. InGaP/GaAs/Ge triple-junction solar cells. [Online]. Available: http://www.emcore.com/assets/photovoltaics/Triple.pdf

[4] P. Wolfs, L. Tang and S. Senini, "Distributed Maximum Power Tracking for High Performance Vehicle Solar Arrays," in *Proc. AUPEC*, 2004.

[5] O. Wasynczuk, "Dynamic Behavior of a Class of Photovoltaic Power Systems," *IEEE Trans. Power App. Syst.*, Vol. 102, No. 9, pp. 3031-3037, Sept. 1983.

[6] B. K. Bose, P. M. Szczesny, and R. L. Steigerwald, "Microcomputer Control of a Residential Power Conditioning System," *IEEE Trans. Ind. Applicat.*, Vol. 21, No. 5, pp. 1182-1191, Sept./Oct. 1985.

[7] K. H. Hussein, I. Muta, T. Hoshino and M. Osakada, "Maximum Photovoltaic Power Tracking: an Algorithm for Rapidly Changing Atmospheric Conditions," in *IEE Proc. Generation, Transmission and Distribution*, Vol. 142, No. 1, pp. 59-64, Jan. 1995.

[8] C. Hua and C. Shen, "Comparative Study of Peak Power Tracking Techniques for Solar Storage System," in *Proc. IEEE APEC*, 1998, pp. 679-685.

[9] C. Hua and C. Shen, "Study of Maximum Power Tracking Techniques and Control of DC/DC Converters for Photovoltaic Power System," in *Proc. IEEE PESC*, 1998, pp. 86-93.

[10] D. P. Hohm and M. E. Ropp, "Comparative Study of Maximum Power Point Tracking Algorithms Using an Experimental, Programmable, Maximum Power Point Tracking Test Bed," in *Proc. IEEE PSC*, 2000, pp. 1699-1702.